

Choosing Promising Sequences of Asteroids

I. S. Grigoriev and M. P. Zapletin

Moscow State University, Moscow, Russia

Received January 15, 2013

Abstract—We consider the problem proposed on the 4th Global Trajectory Optimization Competition (GTOC4).

DOI: 10.1134/S0005117913080055

1. INTRODUCTION

We consider the problem of optimizing the trajectories for a rendezvous mission of a space vehicle (SV) visiting a group of asteroids. SV is controlled through the magnitude and direction of a jet engine thrust (small thrust). The motion of the Earth, asteroids, and the SV occurs in the central Newtonian gravitational field of the Sun. The Earth and asteroids are assumed to be material points moving along predefined elliptic orbits. The SV is launched from Earth, and leaving the Earth is considered in the context of a point sphere of effect with limited extra hyperbolic speed. During the flight, the SV visits (flies by) certain asteroids. In an asteroid flyby, SV and asteroid's locations coincide, but the velocities of the SV and asteroid may be completely different. The trajectory ends when it reaches the last asteroid; both locations and velocities of the SV and the last asteroid must coincide. The problem also takes into account constraints on the time of leaving the Earth, total duration of the flight, and a finite mass. The goal is to maximize the number of visited asteroids.

In this work, we present a solution for the main part of this problem, namely the problem of finding promising sequences of asteroids and time moments of their flybys.

2. PROBLEM SETTING

Differential equations for controllable motion of the SV's center of mass in the Cartesian ecliptic coordinate system look like

$$\begin{aligned} \dot{x} &= u, \quad \dot{y} = v, \quad \dot{z} = w, \quad \dot{m} = -P/C, \\ \dot{u} &= -\frac{\mu x}{r^3} + \frac{P_x}{m} = F_x, \quad \dot{v} = -\frac{\mu y}{r^3} + \frac{P_y}{m} = F_y, \quad \dot{w} = -\frac{\mu z}{r^3} + \frac{P_z}{m} = F_z, \end{aligned} \quad (1)$$

where x, y, z are coordinates, u, v, w are components of the velocity vector, m is the SV's mass, $r = \sqrt{x^2 + y^2 + z^2}$ is the distance from SV to the Sun, $\mu = 1.32712440018 \times 10^{11} \text{ km}^3/\text{s}^2$ is the Sun's gravitational parameter; P_x, P_y, P_z are components of the thrust vector, and $P = \sqrt{P_x^2 + P_y^2 + P_z^2}$ is its magnitude. The magnitude of the thrust vector is bounded:

$$P \equiv \sqrt{P_x^2 + P_y^2 + P_z^2} \leq P_{\max} = 0.135 \text{ N}. \quad (2)$$

$C = P_{\text{unit}} \times g_E$ is the discharge rate of the exhaust blast flow, $P_{\text{unit}} = 3000 \text{ s}$ is the unit thrust, and $g_E = 9.80665 \text{ m/s}^2$ is the gravitational acceleration near the Earth's surface.

The SV's departure from Earth is considered in the method of point sphere of effect with bounded hyperbolic velocity excess. This means that at the moment of departure t_s SV location and Earth location coincides, and the magnitude of the velocity difference vector between SV and Earth does not exceed a given value $\Delta V_E^{\max} = 4$ km/s; the initial SV mass, regardless of the speed of SV leaving the Earth, equals $m_0 = 1500$ kg:

$$\begin{aligned} x(t_s) - x_E(t_s) = 0, \quad y(t_s) - y_E(t_s) = 0, \quad z(t_s) - z_E(t_s) = 0, \\ m(t_s) = m_0, \quad (\Delta V_E)^2 \leq (\Delta V_E^{\max})^2, \end{aligned} \quad (3)$$

where

$$\begin{aligned} \Delta V_E = \sqrt{\Delta u_E^2 + \Delta v_E^2 + \Delta w_E^2}, \\ \Delta u_E = u(t_s) - u_E(t_s), \quad \Delta v_E = v(t_s) - v_E(t_s), \quad \Delta w_E = w(t_s) - w_E(t_s), \end{aligned} \quad (4)$$

$x_E(t)$, $y_E(t)$, $z_E(t)$, $u_E(t)$, $v_E(t)$, $w_E(t)$ represent the location and velocity of the Earth at time moment t .

The moment of departure is chosen from the admissible range:

$$t_s^{\min} \leq t_s \leq t_s^{\max}, \quad (5)$$

where $t_s^{\min} = 57023.0$ MJD (00:00 January 1, 2015), $t_s^{\max} = 61041.0$ MJD (24:00 December 31, 2025).

When flying by an asteroid, SV and asteroid locations coincide, SV and asteroid velocities may differ arbitrarily, and the SV mass is continuous. Formally, the conditions of flying by an asteroid $k = \overline{1, K-1}$ can be represented as

$$\begin{aligned} t_{k-} - t_{k+} = 0, \quad m(t_{k-}) - m(t_{k+}) = 0, \\ x(t_{k-}) - x_{Ak}(t_{k-}) = 0, \quad y(t_{k-}) - y_{Ak}(t_{k-}) = 0, \quad z(t_{k-}) - z_{Ak}(t_{k-}) = 0, \\ x(t_{k+}) - x_{Ak}(t_{k+}) = 0, \quad y(t_{k+}) - y_{Ak}(t_{k+}) = 0, \quad z(t_{k+}) - z_{Ak}(t_{k+}) = 0, \\ u(t_{k-}) - u(t_{k+}) = 0, \quad v(t_{k-}) - v(t_{k+}) = 0, \quad w(t_{k-}) - w(t_{k+}) = 0. \end{aligned} \quad (6)$$

The flight is over when the SV arrives at the last asteroid:

$$\begin{aligned} x(t_f) - x_{AK}(t_f) = 0, \quad y(t_f) - y_{AK}(t_f) = 0, \quad z(t_f) - z_{AK}(t_f) = 0, \\ u(t_f) - u_{AK}(t_f) = 0, \quad v(t_f) - v_{AK}(t_f) = 0, \quad w(t_f) - w_{AK}(t_f) = 0. \end{aligned} \quad (7)$$

The total flight duration and finite mass of the SV are bounded:

$$t_f - t_s \leq t_{\max} = 3652.5 \text{ ED}, \quad (8)$$

$$m(t_f) \geq m_{\min} \equiv 500 \text{ kg}. \quad (9)$$

We maximize, first, the number of asteroids that the SV flies by during its expedition:

$$K \rightarrow \max.$$

Second, among the trajectories that visit the maximal number of asteroids we should choose a trajectory with the largest finite SV mass:

$$m(t_f) \rightarrow \sup. \quad (10)$$

The problem (1)–(10) was proposed in the Fourth Global Trajectory Optimization Competition (GTOC4).¹

To solve this problem, we need to find the optimal sequence of asteroids and maximize SV mass for the chosen sequence of asteroids under the constraints shown above. In what follows, we consider the first part of the problem, i.e., finding the sequence of asteroids.

3. SOLUTION METHOD

The considered problem of visiting a group of asteroids belongs, in terms of [1], to the type of path-routing discrete-continuous problems. The routing part of the problem (in this case, the problem of finding the optimal sequence of visiting asteroids) is discrete in nature. The pathfinding part is to construct a trajectory that satisfies a given set of constraints and minimizes the functional for the chosen sequence of visiting asteroids; it is an optimal control problem with intermediary conditions.

A general approach to solving such problems is to decompose them, i.e., divide the problem into discrete and continuous parts and solve them independently. If we decompose the problem into independent continuous and discrete subproblems, to solve them we further use the Bellman's optimality principle in a suitable modification.

Our solution of the problem at hand was based on the ideas of R. Bellman and N.N. Moiseev. In a series of works of the Yekaterinburg school (see references in [1]), these ideas have been fruitfully developed. These works mostly emphasize theoretical matters; the works are illustrated with low-dimensional model examples, and virtually no attention is paid to overcoming the “curse of dimensionality.” Therefore, we cannot directly apply the algorithms developed there, but, as [1] rightfully notes, “knowledge of the laws of optimal behavior in these low-dimensional (even model) problems may also help to construct approximate algorithms that will be applicable for solving “large” problems.”

Thus, we solve the discrete part of the problem considered in this work with dynamic programming. It would be impossible to make a complete enumeration of all possibilities under these constraints. To solve the problem, we construct a version of the Bellman's function, performing the construction layer by layer and optimizing time and mass expenditure on each step. It is a nontrivial problem to construct, on each of the segments, a flight trajectory satisfying all necessary constraints, and it takes quite some time. Mass automated construction of such trajectories is not implemented yet, so on each segment the trajectory is approximated with a solution of the Lambert problem. It is impossible to enumerate all possible combinations even for a single layer. Therefore, we choose for analysis only “close” asteroids (an idea similar to reachability sets). But even such trajectories are too numerous, so we further select “promising” trajectories and prune the others (an idea similar in spirit to discarding regions upon finding a global extremum). This selection is based on the assumption that the problem has no “bottlenecks.”

Let us now describe all these steps in more detail.

4. THE BUSH OF FLIGHTS

By the flight graph we mean the collection of possible trajectories characterized by the moment when SV launches off the Earth, the sequence of asteroids, and the moments when SV flies by them:

$$\{\text{Earth}, t_s\} \rightarrow \{A_1, t_1\} \rightarrow \{A_2, t_2\} \rightarrow \dots \rightarrow \{A_k, t_k\} \rightarrow \dots \rightarrow \{A_K, t_K\}.$$

¹ Competitions in global trajectory optimizations are described in a special section of the European Space Agency web site <http://www.esa.int/gsp/ACT/mad/op/GTOC/index.htm>.

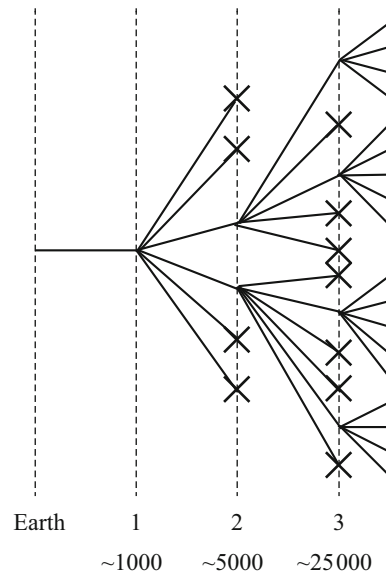


Fig. 1. Flight bush.

These trajectories consist of a collection of passive flight segments (elliptical arcs) from asteroid to asteroid. At the flyby moments, SV velocity changes with a jump, which is interpreted as a result of an impulse impact. The SV mass changes as a result of impulse influences according to the Tsiolkovskii equation.

Here and in what follows A_k (subscripted) denotes the asteroid located at the k th position along the trajectory of visiting asteroids; for different trajectories they may be different. On the other hand, A^i (superscripted) denotes a specific asteroid that may be included or excluded in the flight sequence for different asteroids; if it is included, it may have any admissible position. In total, we consider 1436 near-Earth asteroids in the problem.²

We constructed the graph of possible flights sequentially, layer by layer. Several first stages are schematically depicted on Fig. 1.

4.1. First Stage of the Graph Construction

On the first stage, we solve Lambert problems for flying from the Earth to an asteroid. The launch moments were chosen to cover the admissible range (5) with a step of 10 days. Flight duration from the Earth to the first asteroid was chosen to be from 20 to 60 days with a step of 5 days. We selected minimal duration trajectories among the considered discrete set of durations for which the initial impulse of the Earth did not exceed 4.1 km/s. In case when the Earth's initial impulse ΔV_E (4) does not exceed ΔV_E^{\max} , the SV mass according to (3) was assumed to equal 1500 kg, otherwise the SV mass was found as

$$m(t_{s+}) = m_0 \times \exp(-\max(0, \Delta V_E - \Delta V_E^{\max})/C). \quad (11)$$

On the first stage, we selected about a thousand trajectories.

Note that in the process of selecting the expedition's trajectories we implement a method close to linear in complexity. We need, on one hand, not to miss potentially good trajectories, and on

² The complete list of asteroids considered in this problem and their Keplerian elements are shown on the GTOC4 competition web page: <http://cct.cnes.fr/cct02/gtoc4/index.htm>.

the other hand, minimize the total computations needed. The choice of enumeration parameters resulted from such a compromise.

Let us consider the reasons for choosing these empirical values in more detail.

The 10 day value of the launch grid was chosen to minimize the total amount of computation on the initial stage of the method. Reducing the launch grid's step would add equivalent trajectories, i.e., trajectories with the same sequence of asteroid flyby and a small difference in launch moments from Earth and the corresponding moments of asteroid flybys. A difference in launch moments of less than 10 days with the same sequence of visited asteroids was reduced by optimizing SV mass with respect to the times t_s, t_1, t_2, t_3, t_4 (see Section 4.3) up to the values corresponding to the errors of the optimization method we used.

The choice of trajectory duration of at least 20 days did not prevent us from getting smaller values of flight time in further optimization (see Section 4.3). Restricting the first segment duration to at most 60 days has let us take into account a significant number of trajectories. As we will see later, trajectories with large segment durations were weeded out in subsequent selection of promising branches (see Section 4.3).

The flight duration step of 5 days lets us approximate the set of initial trajectories with sufficient accuracy. If we reduced the step, it would lead to more computation on the first stage of the method and a reduction in the difference of the initial impulse and the 4.1 km/s value. Trajectories with initial impulse exactly equal to 4.1 km/s were not needed in further consideration. Trajectories with initial impulse significantly less than 4 km/s were not prohibited and could be obtained through further optimization of SV mass (see below in Section 4.3). We should note that on the trajectories selected for further analysis the Earth's initial impulse is 1.45271 km/s (see Section 4.5). The initial impulse constraint of 4.1 km/s rather than 4 km/s was chosen due to the need to account for trajectories that continue the flight with an active segment after the initial impulse. At the same time, going significantly over the given constraint ΔV_E^{\max} might mean, first, irrational expenditure of the mass and further pruning of such trajectories as ones that use too much mass (see Section 4.3), and second, significant length of the initial active segment and, consequently, the impossibility to implement such a trajectory with bounded thrust value (2).

4.2. Adding a Level

We assume that we have an impulse trajectory of sequential flight from Earth to an asteroid $\{\text{Earth}, t_s\} \rightarrow \{A_1, t_1\} \rightarrow \{A_2, t_2\} \rightarrow \dots \rightarrow \{A_k, t_k\}$, $k \geq 1$. We are to continue this trajectory with one more segment. To do so, we perform the following steps. At the asteroid flyby time A_k we know the SV approach velocity. The passive approach segment to the last k th asteroid is continued for a given time Δt_k after the flyby, and we determine admissible asteroids A^i (that do not coincide with asteroids A_1, A_2, \dots, A_k that have already been visited in previous stages of the flight) the distance to which does not exceed a given value Δr_k together with the moments t_{k+1}^i when asteroid A^i comes close to the SV (see Fig. 2). Δt_k and Δr_k are parameters of the continuation method, and they may be different for different k . In general, we used the following values in adding the levels: $\Delta r_k = 0.1$ a.u., $\Delta t_k = 100$ days.³

To find target asteroids and flyby moments we used the following algorithm. On the passive trajectory of SV flight, with step 1–2 days we computed the distances between the SV and each admissible asteroid. For each admissible asteroid, we stored the minimum of this discrete set of values and the corresponding time. Thus, at the end of this computation we obtain a set of triples $\{\text{asteroid } A^i, \text{“minimal” distance } r_{k+1}^i, \text{time } t_{k+1}^i\}$. Next we select from this set all records

³ To choose Δt_k we could consider the difference between a certain predefined moment of time and the moment when SV flies by the last asteroid t_k .

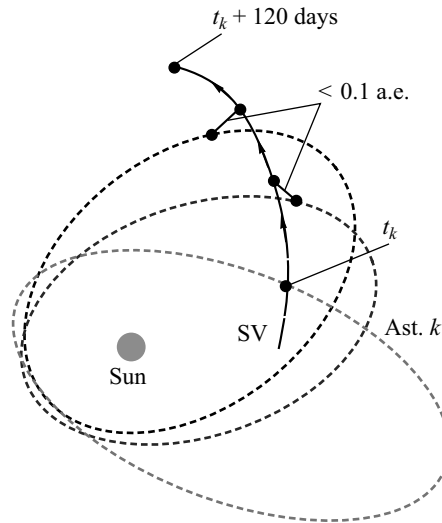


Fig. 2. Adding a level: searching for suitable asteroids.

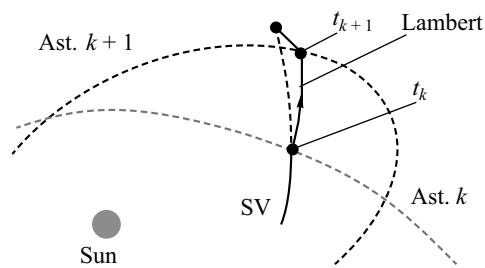


Fig. 3. Adding a level: solving the Lambert problem.

satisfying $r_{k+1}^i < \Delta r_k$ and solve Lambert problems for transitioning from asteroid A_k at time moment t_k to the selected asteroid A^i at time moments t_k^i (see Fig. 3). As a result of this solution, we found the next passive flight segment to the $(k+1)$ th asteroid and the velocity with which SV should leave asteroid A_k . The difference of approach and leaving velocities for the current asteroid determines the value of the impulse for asteroid A_k and, by Tsiolkovskii equation, SV mass near the asteroid A_{k+1} .

Note that in choosing the parameters for the continuation method as $\Delta r_k = 0.1$ a.u., $\Delta t_k = 100$ days, the number of trajectories for the next step increased by 5 to 6 folds on average. The number of trajectories in a stage linearly depends on Δt_k and quadratically depends on Δr_k , and the choice of Δr_k depends on Δt_k . If we increase Δr_k without increasing Δt_k , we only get new inefficient trajectories that are pruned out due to excessive mass expenditure. On the first few stages, we used the duration value $\Delta t_k = 120$ days that was further reduced to $\Delta t_k = 100$ days. The choice of $\Delta t_k = 100$ days was made with regard to a preliminary estimate we had for the possible number of asteroid flybys in 10 years, namely about 40–50 flybys. This number of asteroid flybys corresponds to an average flight duration between asteroids from 73 to 90 days. The most important factor in choosing Δt_k is the following: for the selected values Δr_k , Δt_k , on each stage of graph construction we had a sufficient number of trajectories to further choose promising branches (see Section 4.3) and continue graph construction.

For one and a half thousand trajectories on the K th layer, the algorithm above takes only 15–20 minutes on an average laptop, so we considered this algorithm good enough and did not try to improve its performance.

4.3. Choosing Promising Branches

For the constructed set of trajectories on the $(k + 1)$ th stage we performed intermediate optimization, maximizing the SV mass at the $(k + 1)$ th asteroid with respect to the moments of asteroid flybys. Trajectory on each segment was determined by solving Lambert problems. We used coordinate descent for the optimization. On stages 2 to 5, optimization also included the moment of SV launch from the Earth and all asteroid flyby moments including the last one. Then on several stages optimization was conducted over the three last moments of asteroid flyby and, finally, over two last flyby moments.

Naturally, this is not the fastest optimization method. Among the advantages of this approach we note that it is easy to implement and there are no problems with non-uniqueness of Lambert problems solutions since there is a good initial approximation for a small variation in the time moments. Naturally, we could propose a better modification but the computational resources available to us⁴ let us solve these problems in reasonable time, so we decided to spend the most resources at this stage to choose an efficient condition for trajectory implementability under the given constraints on thrust.

We note the characteristic features of our optimization procedure from the point of view of trajectory graph construction.

If flight times did not change much as a result of optimization, such an optimization was certainly useful. If the flight time to the last asteroid decreased as a result of optimizing the final SV mass, from the point of view of a possibility to add more impulse flight levels and with no regard to the implementability of the trajectory with the existing engine this optimization was also useful. If the flight time to the last asteroid significantly increased as a result of optimizing the final mass for a small gain in the mass, this operation might lead to the loss of a potentially useful branch. The latter problem was sometimes diagnosed, but in the allotted time we did not take any steps towards solving it.

Trajectories with the same sequence of asteroids that initially differ in the moment of SV launch from Earth and, as a result, in the moments of asteroid flyby became equivalent as a result of optimization. We tracked such situations and excluded extra copies of the trajectories from consideration.

A five-fold increase in the total number of branches after adding another level to the graph quickly increases the total amount of computation. We denote by T_k the constraint on the SV flight duration from Earth to the k th asteroid; by m_k , a constraint on the SV mass near the k th asteroid. To reduce the computational load, we performed a selection of “promising” branches, discarding all branches whose flight duration to the k th asteroid exceeded a given T_k or whose final mass was less than a given m_k . Figure 4 shows discarded branches with dashed lines and promising branches with solid lines.

Flight duration constraint for each layer was chosen to exceed the smallest flight duration on a layer by about 300–350 days, and the mass constraint was given by the following relation (see Fig. 5):

$$m_k = -\frac{(920 \text{ kg})}{(10 \text{ yrs})}T_k. \quad (12)$$

⁴ This is the most resource-intensive problem. To solve it, we needed about 8 hours of laptop time (a night) or about one and a half hours (together with synchronization) of the work of 12 computers in a university computer classroom.

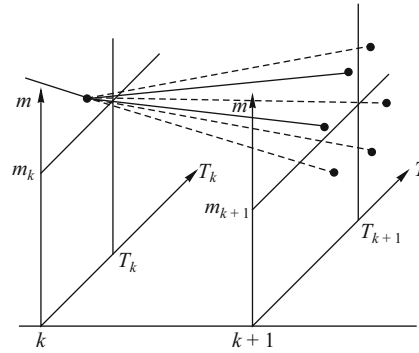


Fig. 4. Choosing promising branches.

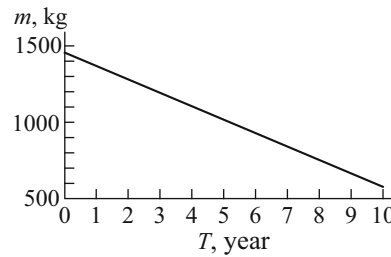
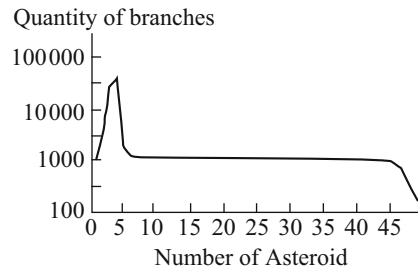

 Fig. 5. Choosing m_k depending on T_k .


Fig. 6. Dynamics of the number of promising branches.

Let us consider the reasons for choosing this dependence in more detail. First, relation (12) takes into account that admissible mass expenditure from 1500 kg to 500 kg lets the engine operate during

$$\begin{aligned} \frac{(1000 \text{ kg}) \times C}{P_{\max}} &= \frac{(1000 \text{ kg}) \times P_{\text{unit}} \times g_E}{P_{\max}} \\ &= \frac{(1000 \text{ kg}) \times (3000 \text{ s}) \times (9.80665 \text{ m/s}^2)}{(0.135 \text{ N})} \approx 7 \text{ years.} \end{aligned}$$

Second, we took into account that approach conditions for the last asteroid presuppose that coordinates and velocities of the SV and the asteroid coincide (7), so we need to have some mass in the reserve to implement this maneuver. Third, it was assumed that the mass expenditure for a trajectory is on average proportional to the flight duration.

Figure 6 shows, in logarithmic scale, an approximate number of promising branches on different stages of constructing the trajectory bush. On initial stages, the time constraint $t_k \leq T_k$ was inactive. The mass constraint $m_k \leq M_k$ also turned out to be quite lenient, so by the fifth layer the total number of promising branches exceeded 12 000. On subsequent layers, the time constraint

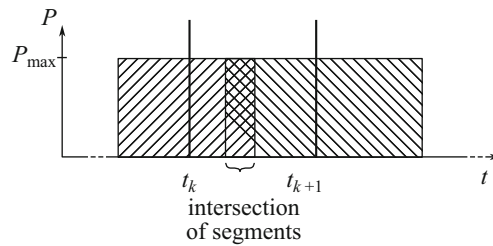


Fig. 7. An overlap of two active segments corresponding to impulse impacts during asteroid flyby and the corresponding solution for a bounded thrust value.

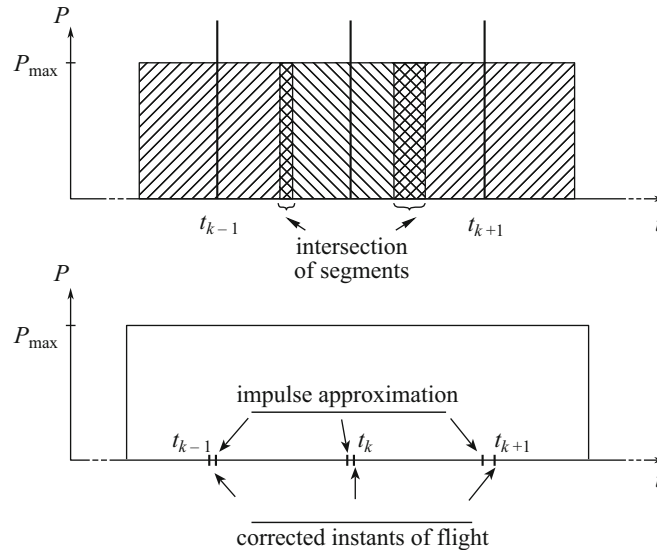


Fig. 8. An overlap of three active segments corresponding to impulse impacts during asteroid flyby and the corresponding solution for a bounded thrust value.

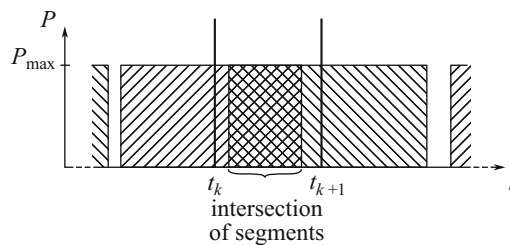


Fig. 9. An overlap of two active segments corresponding to impulse impacts during asteroid flyby that does not let us find a solution for a bounded thrust value.

became active (i.e., the lengthiest trajectories were discarded) and the mass constraint became more strict, so by layer 12 the number of promising branches was reduced to one and a half thousand. On middle stages of constructing the graph of promising trajectories time and mass constraints were active, and the number of promising branches up to layer 45 (virtually up to the very end of the graph construction) remained around 1000–1200. On final stages of the graph construction, the number of promising branches started dropping quickly, and the last layer saw about a hundred admissible branches.

Let us note the main characteristic features of selecting promising branches. Specifying general constraints on flight duration and SV mass and taking into account whether these values are

coherent, also accounted for the implementability of such flights with a priori unbounded thrust value but did not guarantee the implementability of these maneuvers on the existing engine with bounded thrust. As subsequent study showed, we could not implement the resulting promising trajectories under given constraints on thrust value.

The choice of an efficient implementability condition is very important, so over the algorithm's development we spent significant time on trying to choose efficient selection conditions for promising trajectories. For instance, in choosing promising trajectories we could use the "easy implementability" condition that states that active segments corresponding to impulse impacts during asteroid flybys should be disjoint; these conditions were used in asteroid selection in previous similar competitions [2, 3]. However, such conditions would increase the average flight duration between asteroids. An increase in the average flight duration by 10 days gives, for about 40–50 asteroid flybys in a trajectory, an increase in the total duration of the trajectory of about 400–500 days. Taking into account that the average duration of a flight segment between asteroids was slightly above 80 days, this cut the total number of asteroids that could fit into a trajectory by 5–7.

At the same time, for initial segments of certain flyby trajectories for the first ten asteroids we solved the optimal control problem with a constraint on the value of T_{\max} (2). These optimal control problems with intermediate conditions based on the maximum principle [4] reduced to solving multivalued maximum principle boundary problems. Maximum principle boundary problems were solved numerically with the shooting method with a computational scheme similar to multiple shooting method. Our constructions for the initial segments of the extreme solutions showed that an insignificant overlap in two or even three consecutive segments in many cases does not preclude us from constructing Pontryagin extremals (see Figs. 7 and 8). Therefore easy implementability conditions would have to be relaxed.

However, relaxing implementability conditions must, first, not lead to a significant increase in the average flight time between asteroids and, second, discard impossible promising trajectories in a timely fashion. Figure 9 shows a sample sequence of impulse impacts with an overlap in the corresponding active segment approximations in which one ultimately cannot construct a solution under given constraints on thrust value. The main reason for it appears to be the presence of impulse influences shown at the edges of Fig. 9, whose active segment approximations do not intersect with the problematic ones but still do not let us find a solution.

If we choose a condition that increases average flight duration between asteroids and does not track the implementability of a trajectory sufficiently well, it may lead to a deterioration in the final trajectory because we will need to exclude problematic asteroids from the expedition's trajectory.

During the actual problem solving we could not find a more efficient condition for choosing promising trajectories than the simplest one used here. All of the above makes us certain that it did make sense to forgo more complex conditions for choosing promising trajectories during the competition.

4.4. The Final Stage

We add layers to the graph of promising flights while it is possible. Finally, as a result of using the algorithm from Section 4.2 we cannot add a segment to any of the trajectories. Then this stage is considered to be final, and the final SV mass is optimized; this optimization differs from the one shown in Section 4.3 since the objective function now accounts for the last asteroid's impulse. This completes the construction of the graph of promising trajectories.

Note that the total computational load in the proposed algorithm for constructing the graph of promising trajectories in practice linearly depends on the number of asteroids (has linear complexity).

4.5. Results

On the final stage, we selected about a hundred admissible impulse trajectories that fly by 48 asteroids and arrive at the 49th. For further analysis we selected 7 flights that were best with respect to duration and mass. All trajectories chosen for further consideration (Fig. 10) started at the same

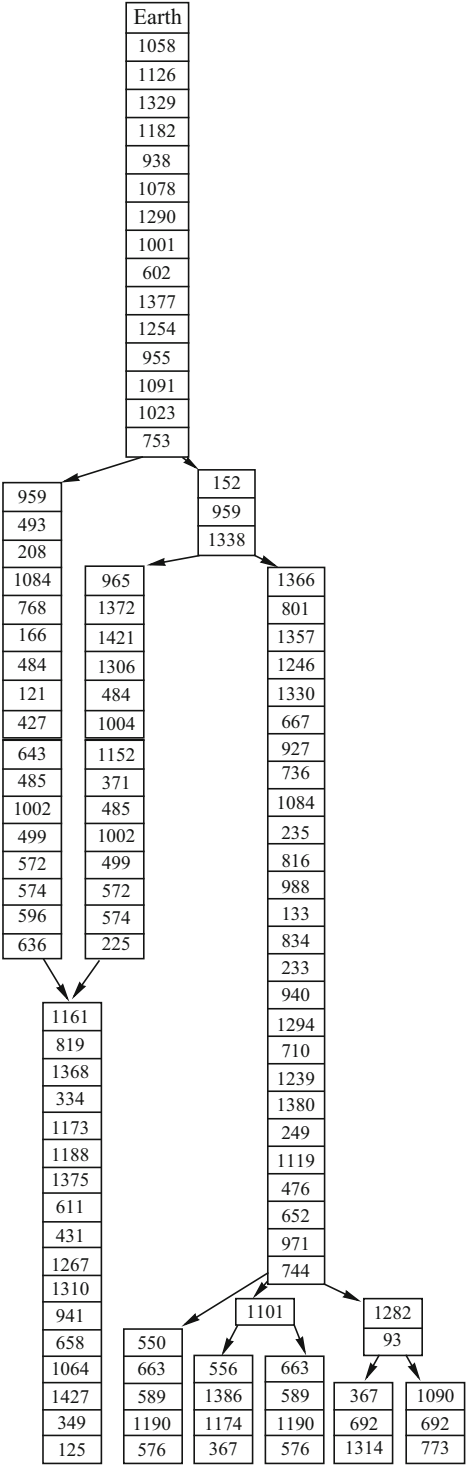


Fig. 10. Seven chosen trajectories.

Best trajectory for SV flight

| no. | t | $m(t_+)$ | Asteroid | no. | t | $m(t_+)$ | Asteroid |
|-----|----------|----------|----------|-----|----------|----------|----------|
| 0 | 58676.40 | 1500.00 | 0 | 1 | 58731.65 | 1487.47 | 1058 |
| 2 | 58801.45 | 1455.53 | 1126 | 3 | 58866.95 | 1447.41 | 1329 |
| 4 | 58973.95 | 1433.87 | 1182 | 5 | 59084.55 | 1415.27 | 938 |
| 6 | 59119.45 | 1407.21 | 1078 | 7 | 59221.75 | 1369.68 | 1290 |
| 8 | 59326.95 | 1362.41 | 1001 | 9 | 59366.25 | 1332.88 | 602 |
| 10 | 59419.55 | 1317.69 | 1377 | 11 | 59520.05 | 1298.40 | 1254 |
| 12 | 59586.25 | 1289.05 | 955 | 13 | 59685.15 | 1287.81 | 1091 |
| 14 | 59746.75 | 1277.76 | 1023 | 15 | 59863.25 | 1242.19 | 753 |
| 16 | 59901.25 | 1227.92 | 152 | 17 | 59955.85 | 1219.21 | 959 |
| 18 | 60078.75 | 1189.08 | 1338 | 19 | 60157.05 | 1172.01 | 1366 |
| 20 | 60233.95 | 1142.62 | 801 | 21 | 60334.75 | 1126.08 | 1357 |
| 22 | 60422.75 | 1119.34 | 1246 | 23 | 60507.25 | 1101.87 | 1330 |
| 24 | 60549.75 | 1093.41 | 667 | 25 | 60601.15 | 1082.33 | 927 |
| 26 | 60665.25 | 1073.82 | 736 | 27 | 60796.75 | 1064.09 | 1084 |
| 28 | 60897.85 | 1047.89 | 235 | 29 | 60938.15 | 1031.98 | 816 |
| 30 | 61054.35 | 996.52 | 988 | 31 | 61082.15 | 979.77 | 133 |
| 32 | 61110.35 | 960.43 | 834 | 33 | 61201.65 | 955.95 | 223 |
| 34 | 61221.35 | 934.20 | 940 | 35 | 61285.55 | 925.47 | 1294 |
| 36 | 61377.65 | 907.40 | 710 | 37 | 61441.75 | 901.59 | 1239 |
| 38 | 61486.75 | 895.42 | 1380 | 39 | 61562.75 | 860.65 | 249 |
| 40 | 61646.75 | 839.49 | 1119 | 41 | 61727.45 | 826.31 | 476 |
| 42 | 61806.65 | 785.42 | 652 | 43 | 61867.75 | 778.96 | 971 |
| 44 | 61921.85 | 767.85 | 744 | 45 | 61979.55 | 763.83 | 1101 |
| 46 | 62057.15 | 723.42 | 556 | 47 | 62105.85 | 705.79 | 1386 |
| 48 | 62151.65 | 703.19 | 1174 | 49 | 62261.25 | 616.45 | 367 |

launch moment $t_s = 58676.40$ MJD from Earth with the same velocity of SV leaving the Earth: $\Delta u_E = -0.205100$ km/s, $\Delta v_E = -1.436312$ km/s, $\Delta w_E = 0.072829$ km/s, $\Delta V_E = 1.452708$ km/s. Flight segments to the first 15 asteroids and the chosen asteroids completely coincide. Five trajectories differ only in the segments of visiting the last asteroid; two trajectories have common segments for visiting the last 16 asteroids and differ in chains of visits to the intermediate 18 asteroids. Note that the selected sequence of asteroids had a wide range of parameters: e (0.07–0.89); a (0.76–2.61 a.e.); i (0.29–37.3 grad.). The Table lists SV masses after impulse influences during each asteroid flyby for the best trajectory. Taking into account that trajectories for flying from asteroid to asteroid are passive segments, the values of SV mass shown in the Table let us find, by Tsiolkovskii equation and without solving the Lambert problems, the values of impulse influences for each of the asteroids.

5. CONCLUSION

After finding a promising sequence of asteroids and the moments of visiting them, we constructed a trajectory that would satisfy all constraints of the original problem (1)–(9) and maximize SV mass at the end of the trajectory (10). At the beginning of the next stage of the solution the problem was formalized as a problem in an impulse setting. The moments for asteroid flybys were refined, and we found Lagrange multipliers (adjoint variables) corresponding to the chosen trajectory. Then we passed to a trajectory with bounded thrust. The resulting trajectory placed first at the Global Trajectory Optimization Competition. We plan to devote our next article to a description of these steps.

REFERENCES

1. Chentsov, A.G., *Ekstremal'nye zadachi marshrutizatsii i raspredeleniya zadaniy: voprosy teorii* (Problems of the Theory of Extremal Routing and Task Assignment Problems), Izhevsk: NITs "Regulyarnaya i Khaoticheskaya Dinamika," 2008.
2. Grigorev, I.S. and Zapletin, M.P., On One Optimization Problem for Trajectories of SV Visiting a Group of Asteroids, *Kosm. Issled.*, 2009, vol. 47, no. 5, pp. 460–470.
3. Grigoriev, I.S. and Zapletin, M.P., Constructing Pontryagin Extremals for the Optimal Control Problem of Asteroid Fly-By, *Autom. Remote Control*, 2009, vol. 70, no. 9, pp. 1499–1513.
4. Grigorev, I.S. and Grigorev, K.G., On Maximum Principle Conditions in Optimal Control Problems for a Collection of Dynamical Systems and Their Application to Solving Optimal Control Problems for the Motion of Spacecraft, *Kosm. Issled.*, 2003, vol. 41, no. 3, pp. 307–331.

This paper was recommended for publication by V.N. Tkhai, a member of the Editorial Board